Aerosol Science and Technology, 40:373–388, 2006

ISSN: 0278-6826 print / 1521-7388 online
DOI: 10.1080/02786820600631896

Characteristics of Fine Particle Growth Events Observed Above a Forested Ecosystem in the Sierra Nevada Mountains of California

Melissa M. Lunden,[1] Douglas R. Black,[1] Megan McKay,[2] Kenneth L. Revzan,[1] Allen H. Goldstein,[1,2] and Nancy J. Brown[1]

[1]*Environmental Energy Technologies Division, Lawrence Berkeley National Laboratory, 1 Cyclotron Rd., Berkeley, California, USA*

[2]*ESPM—Ecosystem Sciences, University of California, Berkeley, California, USA*

Atmospheric aerosols from natural and anthropogenic processes have both primary and secondary origins, and can influence human health, visibility, and climate. One key process affecting atmospheric concentrations of aerosols is the formation of new particles and their subsequent growth to larger particle sizes. A field study was conducted at the Blodgett Forest Research Station in the Sierra Nevada Mountains of California from May through September of 2002 to examine the effect of biogenic volatile organic compounds on aerosol formation and processing. The study included in-situ measurements of concentration and biosphere-atmosphere flux of VOCs, ozone, aerosol size distribution, aerosol physical and optical properties, and meteorological variables. Fine particle growth events were observed on approximately 30 percent of the 107 days with complete size distribution data. Average particle growth rates measured during these events were 3.8 $\pm$ 1.9 nm hr^{-1}. Correlations between aerosol properties, trace gas concentrations, and meteorological measurements were analyzed to determine conditions conducive to fine particle growth events. Growth events were typically observed on days with a lesser degree of anthropogenic influence, as indicated by lower concentrations of black carbon, carbon monoxide, and total aerosol volume. Days with growth events also had lower temperatures, increased wind speeds, and larger momentum flux. Measurements of ozone concentrations and ozone flux indicate that gas phase oxidation of biogenic volatile organic compounds occur in the canopy, strongly suggesting that a significant portion of the material responsible for the observed particle growth are oxidation products of naturally emitted very reactive organic compounds.

Received 30 March 2005; accepted 10 February 2006.

This research was supported by the Assistant Secretary for Fossil Energy, Office of Natural Gas and Petroleum Technology, through the National Petroleum Technology Office under U.S. Department of Energy Contract No. DE-AC03-76SF00098 and the Independent Petroleum Association of Mountain States. The authors are grateful for the efforts of other colleagues who have provided technical assistance; Dennis Debartalomeo, Ken Hom, Erin McNamara and Toshi Hotchi of LBNL, and Bob Heald and the Blodgett forest crew for operational support.

Address correspondence to Melissa M. Lunden, Environmental Energy Technologies Division, Lawrence Berkeley National Laboratory, 1 Cyclotron Rd., Berkeley, CA 94720, USA. E-mail: MMLunden@lbl.gov

INTRODUCTION

Aerosols can be found throughout the Earth's atmosphere, and result from a number of processes, both natural and anthropogenic. These processes involve both direct emission from the source and secondary formation in the atmosphere by gas-to-particle conversion mechanisms. Atmospheric aerosols have received considerable attention lately due to increased recognition of their influence on human health, visibility, and global climate. Understanding these effects requires knowledge concerning the formation of particles in the atmosphere, their transport and transformation in the atmosphere, and their removal mechanisms.

It is important to understand the formation and processing of atmospheric aerosols in regions where anthropogenic emissions interact with those from rural or remote regions. The biosphere can be a significant source of aerosols. In their 2001 report, Intergovernmental Panel on Climate Change (IPCC) estimates global biogenically derived secondary organic aerosols (SOA) are in the range of 8 to 40 Tg yr^{-1}, while those from anthropogenic precursors range from 0.3 to 1.8 Tg yr^{-1} (IPCC 2001). As urban areas continue to grow, the interaction between their emissions and those from the rural biosphere is of increased importance. Terrestrial vegetation releases a number of reactive organic compounds, such as isoprene, mono- and sesquiterpenes into the atmosphere. The total annual global biogenic organic emissions are estimated to be 1150 Tg yr^{-1}, while the estimate for total anthropogenic emissions is 142 Tg yr^{-1} (Seinfeld and Pandis 1998). When anthropogenic emissions are advected into these rural regions, they alter the biosphere-atmosphere interaction between organic gases and trace gas species such as ozone (Dreyfus et al. 2002). There is limited information about how the presence of anthropogenic emissions affects the efficiency

of SOA production involving biogenic precursors. Kanakidou et al. (2000) report that increased emissions of NO_x may result in a possible 3 to 4 fold increase in biogenic organic aerosol production since pre-industrial times.

A key process affecting atmospheric concentrations of aerosols is the formation of new particles and their subsequent growth to larger sizes. Since atmospheric aerosols are constantly lost due to scavenging by larger particles, dry deposition, and removal by precipitation, new sources are required to maintain observed particle concentrations in the troposphere. Several investigators have observed particle formation events in the continental boundary layer, which are characterized by the observation of ultra-fine particles detected at a few nanometers in size, accompanied by growth to the 100 nm size range within 1 to 2 days (Kulmala et al. 2004). These observations span a number of different environments from the remote boreal forest (Makela et al. 1997; Kulmala et al. 1998), coastal environments in Europe (O'Dowd et al. 1999), forested ecosystems in mountainous regions (Weber et al. 1997), and in urban regions of the United States (Woo et al. 2001; Stainer et al. 2004.) Particle formation events have also been observed to occur over large spatial scales, implying that the processes driving these events are regional, rather than local, in nature (Vana et al. 2004; Stainer et al. 2004).

Two steps are necessary for the production of new particles in the atmosphere. The first is the formation of stable nuclei in the atmosphere, and the second is the growth of those nuclei to larger particle sizes. The chemical species responsible for nuclei formation and subsequent growth are not necessarily the same. Current aerosol instrumentation does not allow for direct measurement of particles below 3 nm, therefore inferences concerning the mechanisms behind the formation of these nuclei are made by concomitant observations of gas phase precursors and ultra-fine particles (Weber et al. 1997; Stainer et al. 2004). A number of mechanisms have been proposed for the formation of nuclei including homogeneous binary nucleation of water and sulfuric acid (Weber et al. 1999), homogeneous ternary nucleation of ammonia, water, and sulfuric acid (Kulmala et al. 2002), homogeneous nucleation of low vapor pressure organic compounds (O'Dowd et al. 2002), and ion induced nucleation (Yu and Turco 2000). With rare exception, most observed growth events occur during the daytime, suggesting that photochemistry is central to the process. Much of the recent work has indicated the involvement of sulfuric acid (H_2SO_4) in nucleation. Measurements of clusters during nucleation events (Weber et al. 1997) showed strong evidence of an association between sulfuric acid and nucleation and many recent observations have shown correlations between growth events and elevated SO_2 concentrations (Woo et al. 2001; Steiner et al. 2004; Dunn et al. 2004).

The growth of the fine mode aerosol from these incipient nuclei will occur when atmospheric precursor concentrations and meteorological conditions are favorable. Most observations support the idea that nucleation and subsequent particle growth are uncoupled (Kulmala et al. 2004). For instance, measured concentrations of gaseous sulfuric acid concentrations do not, in general, account for the observed particle growth (Weber et al. 1997; Stainer et al. 2004). While it is generally thought that organic vapors do not, in general, participate in nucleation, the condensation of low vapor pressure oxidation products of organic gases are likely to contribute to the growth of nucleated particles (Kulmala 2004). There is some evidence of the role of biogenic emissions in aerosol formation (Kavouras et al. 1998; Becker et al. 1999; O'Dowd et al. 2002; Zhang et al. 2004). Recent measurements performed in Pittsburgh (Zhang et al. 2004) that combined gas and aerosol instrumentation with particle mass spectrometers provided evidence that oxidation products of organic species contribute significantly to particle growth after new particle formation, particularly as the day proceeds and photochemistry becomes more intense. Moreover, there is recent experimental evidence that acidic precursors can enhance the amount of organic material that partitions into the particle phase (Jang et al. 2002; Zhang and Wexler 2002).

Our objective is to understand the conditions leading to observed growth of fine particles in a forested environment, to investigate the influence of anthropogenic emissions on these growth events, and to examine evidence for oxidation products of biogenic volatile organic compounds (VOCs) contributing to this aerosol growth. We conducted aerosol characterization measurements in concert with measurements of the gas phase concentrations of biogenic and anthropogenic VOCs and meteorological variables for several months at the University of California Blodgett Forest Research Station. Growth of ultrafine particles was often, but not always, observed. In this paper, we report on the relationships between particle growth events and the observed aerosol properties, trace gas concentrations, and meteorology. Average diurnal behavior of these variables is examined to understand the influence of anthropogenic pollutants at the site, and the correlations between anthropogenic emissions and particle growth events. Observed growth rates for this site, a Western United States boreal forest, is compared with those measured elsewhere. A more mechanistic investigation of the detailed processes connecting the observed particle growth with biogenic VOC concentrations and anthropogenic pollutants will be discussed in a subsequent manuscript.

EXPERIMENTAL METHODS

Site Description

The field site is near the Blodgett Forest Research Station (38°53′42.9″N, 120°37′57.9″W, 1315 m) on the western slope of the Sierra Nevada Mountains in California, approximately 75 km northeast of Sacramento. Measurements at the site were established in 1997 (Lamanna and Goldstein 1999; Goldstein et al. 2000). The site is characterized by a Mediterranean climate, with warm dry summers and rainfall between September through May. The site is an evenly aged Ponderosa Pine

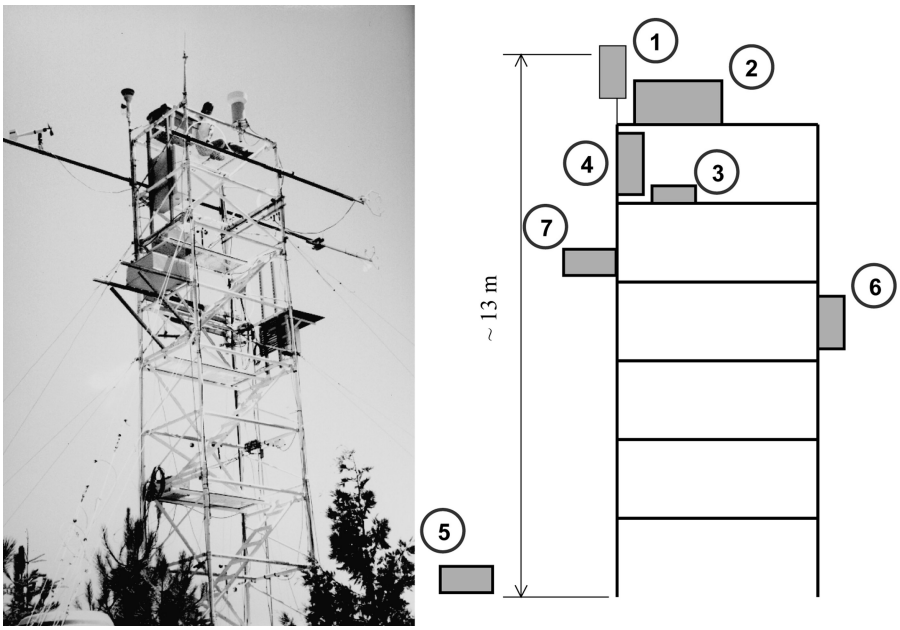

FIG. 1. Picture of the tower at the Blodgett Forest Field Site. The boxes mounted on the tower contain the aerosol equipment. The schematic shows the locations of the aerosol instrumentation on the tower. The instruments are as indicated: (1) 2.5 mm cyclone inlet, (2) aethalometer, (3) condensation particle counter, (4) scanning mobility particle scanner, (5) optical particle sizer, (6) nephelometer, and (7) filter samplers.

plantation planted in 1990 and owned by Sierra Pacific Industries. Measurements were conducted using a 12-m walk-up tower, shown in Figure 1.

The topography and typical wind trajectories are shown schematically in Figure 2. The meteorology at the site is quite consistent during the summer. The predominant daytime airmass trajectory is the northeast direction, carrying anthropogenic pollutants downwind from Sacramento and the agricultural Central Valley of California. During the evening, a drainage flow moves cleaner air downslope from the Sierra Nevada Mountains.

The site is powered by a diesel generator located ~130 m to the northwest of the tower. During the day, the flow from the west is strong enough that plumes from the generator are rarely observed. At night the winds are weaker, and an occasional plume of short duration is observed. These data points can be identified by brief increases in black carbon and total particle concentrations.

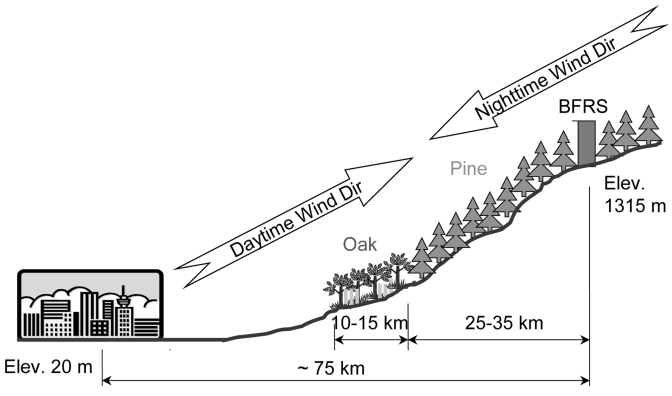

FIG. 2. Schematic showing the location of the Blodgett Forest Research Station in relation to Sacramento and regional vegetation. The predominant wind directions are also indicated on the figure.

Aerosol Measurements

The physical properties of the aerosols at the site were measured using a variety of instruments. The optical properties of the aerosol were measured using an aethelometer (Model. AE2, McGee Scientific, Berkeley, CA) and an integrating nephelometer (NGN-2, OPTEC, Inc., MI). An integrated measure of the aerosol number concentration was provided by a condensation particle counter (CPC, Model 3022A, TSI Inc., Shoreview, MN). Particle size distributions at the site were measured using an optical particle counter (OPC, Lasair Model 1003, Particle Measurement Systems, Boulder, CO) providing size distributions from 0.1 to 10 μm, and a scanning mobility particle sizer (SMPS) providing size distributions between 10 and 400 nm. The SMPS system utilized a differential mobility analyzer (Model 3071A, TSI Inc.) coupled with a CPC (Model 3760, TSI Inc.) as a detector. All instruments except the OPC were mounted on the tower. The OPC was located in an adjacent instrument container. A schematic of the instrument placement on the tower is shown in Figure 1. The air was sampled at 16.7 L min^{-1} through a PM10 inlet followed by a PM2.5 sharp cut cyclone (Models 57-000596 and 57-005896, respectively, Rupprecht & Patashnick Co. Inc., East Greenbush, NY). The inlet was mounted above the top of the tower at a height of approximately 13 m. Sample flows for the

aethalometer, CPC, SMPS, and OPC were isokinetically sampled from this main flow. Measurements were recorded from 9 May to 14 November in 2002, with the exception of the SMPS, which was started on 29 May. Measurements from the CPC, SMPS, OPC, and nephelometer were recorded every 2 minutes, while those from the aethalometer were recorded every 5 minutes.

The aethelometer measures light absorption of the aerosol, b_{abs}, using a filter-based light transmission technique. (Hansen 1984) The instrument measures decreases in transmitted light through an increasingly particle-laden filter. Black carbon (BC) is the insoluble, most resistant to heating, graphitic, and strongly light absorbing component of the aerosol mass. The aethalometer used for this study measured light absorption at two wavelengths, 880 nm (near IR) and 350 nm (near UV). BC is believed to be the only aerosol component that absorbs in the near infrared spectral region, so measured transmission of 880 nm wavelength light is used to determine BC concentration. An empirically derived calibration equation is used to estimate the mass concentration of BC in air (in μg m^{-3}) from the measured decrease in light transmission (Gundel et al. 1984). Blue and near ultraviolet light transmission measurements are used to indicate the presence of aerosol materials that absorb in these spectral regions, such as mineral dust (d'Almeida 1987) and some types of organic compounds. (Kirchstetter 2004; Bond 2001) The flow rate through the instrument was 4 L min^{-1}.

The nephelometer measures the light scattering coefficient, b_{scat}, at an effective wavelength of 550 nm. The instrument, described in more detail by Molenar et al. (1989), has an open air design, allowing the air to pass through a large opening in the side of the instrument. This design minimizes the changes in relative humidity and temperature that has lead to underestimated scattering measurements in other nephelometers. Because the instrument is open, it allows a wide range of particle sizes to pass through it, including particles >2.5 μm. The cutpoint of the instrument has not been characterized.

The SMPS system measures aerosol size distributions by classifying particles based upon their electrical mobility. Particles entering the DMA are passed through a Kr-85 source that is used to generate bipolar gas ions that attach to the particles. The charged particles are classified by their drift velocity in an electrical field—only particles with a specific charge to mass ratio are extracted from the instrument and counted with a CNC. The size distribution is obtained by exponentially ramping the voltage applied to the DMA (Wang and Flagan 1990). The SMPS system at the Blodgett field location sampled aerosol at a flow rate of 0.7 L min^{-1}. Utilizing a sheath flow rate in the mobility classifier of 7 L min^{-1}, a full voltage scan of the instrument resulted in size distributions from 10 nm to 400 nm. The SMPS system was controlled using Labview software and National Instruments control boards. One complete size distribution was obtained in a little over 1 minute using software developed by Donald Collins of Texas A&M University and Patrick Chuang of the Univeristy of California at Santa Cruz. The inversion program used to process the raw data was based on that presented by Collins et al. (2002).

Meteorological and Other Measurements

Meteorological parameters such as air temperature, humidity, wind speed and direction, and net and photosynthetically active radiation (PAR) were measured continuously and stored as 30 minute averages. Meteorological data and trace gas mixing ratios and fluxes (CO_2, H_2O, O_3, and hydrocarbons) were measured approximately 5–6 m above the average tree height (Goldstein et al. 2000).

Total ozone flux was measured using the eddy covariance method (Kurpius et al. 2002). Wind speed was measured with a three-axis sonic anemometer (ATI Electronics, Inc.) at 10 Hz. Ozone was measured with a closed-path, fast-response chemiluminescent instrument (NOAA-ATDD) at 10 Hz and a slower-response UV photometric O_3 analyzer (Dasabi 1008-RS) was used as a stable residence. Total ozone flux was apportioned into deposition flux due to stomatal and non-stomatal surface uptake and gas-phase chemistry within the forest canopy as reported in Kurpius and Goldstein (2003).

Data Reduction

It was necessary to remove data associated with periods when the measurements were dominated by emissions from the generator. As noted previously, during the night when the winds are weak, plumes of particulate emissions from the generator can be observed in the aerosol data. Diesel generators emit large concentrations of small ($<$100 nm) carbonaceous particles. These emissions are reflected in the data by brief increases in black and total particle concentrations, as well as the appearance of a smaller mode in the size distribution data. Previous measurements of VOCs at the site indicate that the emissions from the generator influence the sampling platform approximately 5% of the time, and occurred almost exclusively at night (Goldstein et al. 2000).

In order to systematically remove the influence of the diesel generator emissions from the data set, a series of data rejection routines was developed that test for quick, short, large-scale departures from the general data stream. The data rejection routines were applied to data from the CPC, aethalometer, and SMPS. For the SMPS data set, the filter was first applied to a total number concentration data set calculated by integration of the size distribution data, and resulted in the identification of time intervals where the data should be removed. A mask of these filtered times was then applied to the matrix of time-resolved size distribution data.

RESULTS AND DISCUSSION

Diurnal Profiles

Mean diurnal profiles were calculated from the aerosol, meteorological, and trace gas data. The calculations were performed

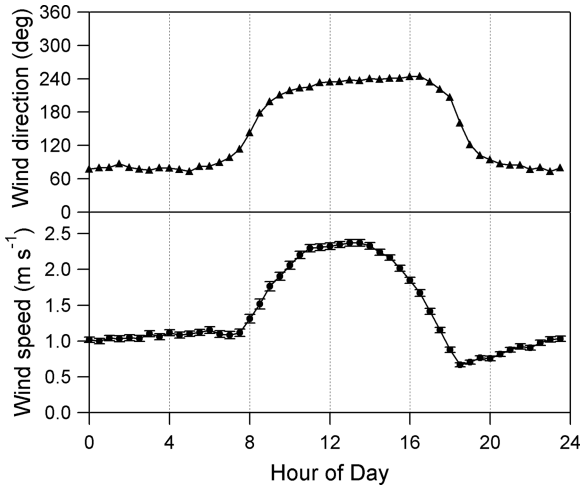

FIG. 3. Diurnal patterns of wind speed and wind direction at the Blodgett measurement site calculated for days between 29 May and 30 September. The error bars denote the standard error of the mean.

on a subset of the data during which the SMPS system was operational, between 29 May and 30 September. This time period is essentially the dry summer period in California, with rare rainfall and limited cloud cover. The diurnal averages calculated from the data set did not vary significantly from those calculated for the summer months of July through September.

The averaged diurnal profiles for wind speed and wind direction are shown in Figure 3, clearly indicating the diurnal upslope/downslope flow pattern that are prevalent throughout most of the western Sierra Nevada Mountains. As the day proceeds, heating of the air in the Central Valley results in daytime winds that push the air upslope along the mountains. Between 1600 and 1800 PST, the flow is reversed as cooling air descends back into the valley. This consistent meteorology aids in interpreting results from the site because, with rare exception, the trajectory of the air mass arriving at the site as the day proceeds comes from a narrow range of directions. In addition, cloud cover is very infrequent during the summer, ensuring that most days experience similar levels of radiation intensity that gradually vary seasonally with sun angle. Thus, day-to-day differences in the levels of radiation available to drive reactions will not have as great an affect on differences in observed growth events as those due to other meteorological factors.

The diurnal pattern in ozone concentration shows a morning dip in concentration after sunrise followed by an increase to an afternoon maximum (Figure 4b). This pattern is the typical pattern observed at this location (Kurpius et al. 2002). In their work, the morning decrease in ozone concentration was attributed to increased stomatal activity at sunrise, taking up ozone when the air is relatively stable with little vertical or horizontal mixing. However, recent ozone flux measurements indicate significant ozone loss within the canopy due to gas-phase chemical reaction (Kurpius and Goldstein 2003). This conclusion was

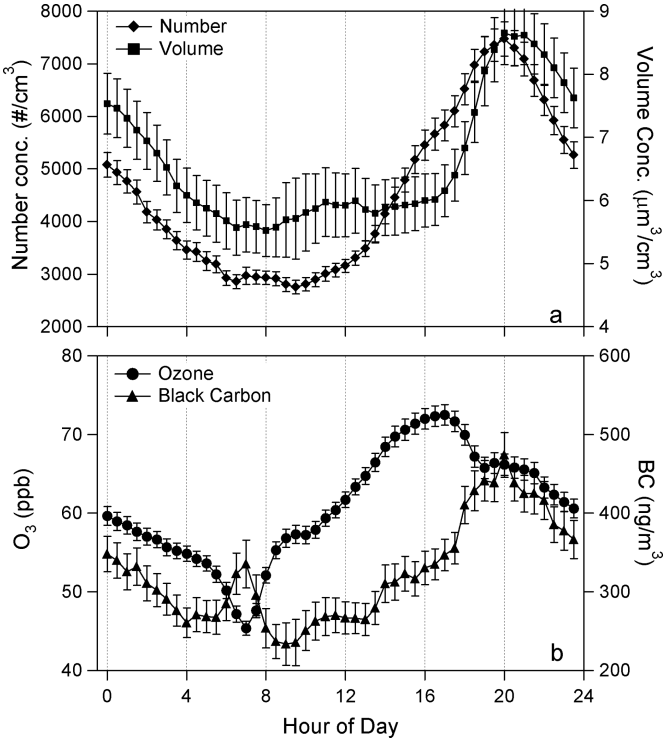

FIG. 4. Diurnal patterns of (a) integrated particle number and volume concentration calculated for the size range 10 to 410 nm from the measured mobility distributions and (b) ozone and black carbon concentration calculated for days between 29 May and 30 September. The error bars denote the standard error of the mean.

recently strengthened by VOC measurements that showed a correlation between highly reactive, light dependent terpene compounds that are emitted upon sunrise and the observed decrease in ozone concentration, suggesting that some of the morning decrease in ozone is likely due to chemical reactions with terpenes in the canopy (Lee et al. 2005). As vertical mixing increases, the ozone concentration rebounds (Figure 4b). The late afternoon increase is due to the transport of ozone and its precursors from the Sacramento urban area to the Blodgett field site (Dillon et al. 2002).

Figure 4b also shows the mean diurnal pattern for black carbon (BC) concentrations. BC serves as an excellent tracer for anthropogenic aerosol emissions since it is emitted from combustion sources as an aerosol and undergoes limited chemical transformation in the atmosphere (Hansen and Rosen 1985; Goldberg 1985). The BC concentration shows a spike in concentration that begins approximately a half hour after the ozone begins to decrease, and peaks at approximately 0700 PST. The Blodgett field site is located 25 to 35 kilometers from the closest interstates (I-50 and I-80, respectively), and approximately 15 km from the nearest town (Georgetown, CA, population $\sim$1000). Emissions from these sources would take some time to arrive at the site, particularly in the early morning when wind speeds are low and the wind direction has not yet shifted

to the daytime upslope direction. Therefore, it is unlikely that the increase in concentration is due to emissions from morning traffic. While the diesel generator providing energy for the site might seem a likely contributor this spike in measured BC concentrations, we believe that this is not the case. As discussed previously, direct emissions from the generator are easy to detect, and we feel that their contribution to measured BC concentrations were successfully removed from the data set. It may be possible, however, that emissions from the generator linger near the site during the evening when mixing heights and wind speeds are low and affect the site in the morning as the atmosphere becomes more active and the boundary layer begins to grow. Therefore, while this morning spike is intriguing, it is not apparent at present where this black carbon is coming from.

The increase in BC concentration just after noon is a result of emissions from the Central Valley reaching the site. The median daytime local winds at the Blodgett field site indicate that it takes approximately 7 hours for an air parcel to travel between downtown Sacramento and Blodgett (Dillon et al. 2002). BC concentrations continue to rise throughout the afternoon as emissions are advected to the site from the valley. Local emissions are likely to add to the later afternoon and evening concentrations, particularly from wood burning that is a major source of residential heat in the area.

The diurnal profiles of particle number and particle volume, calculated from the mobility distributions, are shown in Figure 4a. Note that there is not a strong increase in either the number or volume concentration that corresponds to the increase in the BC concentration in Figure 4b, although a slight increase in number concentration can be seen occurring at approximately the same time. The number concentration increases fairly rapidly after noon as pollutants from the Sacramento region begin to arrive at the site. The increase in number concentration during the afternoon also reflects the growth of nuclei-mode particles near the measurement site. The particle volume concentration increases much more moderately as the day proceeds. The increase in the morning is likely due to the formation of secondary inorganic aerosols such as ammonium sulfate and ammonium nitrate, both important species in Calfornia. Ammonium nitrate formation in particular has been shown to peak in during the morning to midday timeframe at other locations in the San Joaquin Valley, and this peak has been observed to correspond with peak gas phase ammonia concentrations. (Stolzenburg and Hering 2000; Hering et al. 2001; Lunden et al. 2003). The volume concentration increases dramatically after 1700 PST, which corresponds to sharp increases in the BC concentrations. Indeed the correlation between particle volume and black carbon is relatively high at 0.8. The volume increase is partially due to advection of pollution from the Sacramento urban area and local emissions, and may also be due to modest hygroscopic growth of the aerosol attributed to the relative humidity increase observed in the late afternoon as air temperature declines.

Particle Growth Events

Fine particle growth events were observed on approximately 1/3 of days at the Blodgett location. During these growth events, newly formed particles of size 10 to 20 nm appear around noon and grow at the rate of a few nanometers per hour, reaching sizes between 60 to 80 nm in the evening. A typical event is shown in Figure 5. These growth events are similar to those observed by a number of other investigations (Kulmala et al. 2004). Figure 5a shows the size distribution as measured by the SMPS; the ordinate displays particle diameter, the abscissa the time of day, and the color scale indicates the value of the particle size distribution in a particular size range. Figures 5b through 5d show the size distribution at the onset, during, and after the appearance of the growth event. The size distribution at onset of the growth event has a mean diameter of 100 nm (Figure 5b). A small mode is just visible as a hump on the distribution, with a fitted mean diameter of 21 nm. As the growth event proceeds, the size distribution becomes bimodal as the nuclei mode grows larger. In Figure 5c, the smaller mode has grown to a mean diameter of 24 nm. As the nuclei mode grows into the Aitken mode, it becomes the dominant mode in the distribution (Figure 5d) and eventually leads to a size distribution that is largely unimodal.

Before proceeding with any analysis of the observed growth events, it is important to understand the limitations of a single sampling location when analyzing size distribution data. Observations at fixed position in space observe different aerosols at different times and not the same aerosol evolving in time, which would require following the same air parcel in a Lagrangian frame. Therefore, most analyses of growth events use a Eularian approach to investigate processes as if the aerosol was growing at the measurement location, assuming that measurements performed at a single location will reveal important insights into the aerosol growth mechanisms (Kulmala et al. 1998; Clement et al. 2001; Weber et al. 1997). The import assumption in using this approach is that the air mass in which the aerosol is being sampled is relatively homogeneous over large spatial scales (McMurry and Wilson 1982; Juotzaitis et al. 1996). Most particle formation and growth events observed at a stationary location show sustained growth over several hours, which implies that the nucleation of new particles occurs over large spatial scales and the growth of these particle by condensation and/or coagulation also occurs throughout the air mass, otherwise there would be no pattern to the observations. Particle formation events have often been observed to occur over large spatial scales, as much as several hundred kilometers, which implies some degree of homogeneity in the air mass that affect the nucleation and/or growth processes (Kulmala 2001; Vana et al. 2004; Stainer et al. 2004). Vana et al. (2004) showed that correlations between air mass trajectories, meteorology, and growth events observed at three stations located in Finland and Estonia imply that the fine particle formation events are a synoptic-scale phenomenon.

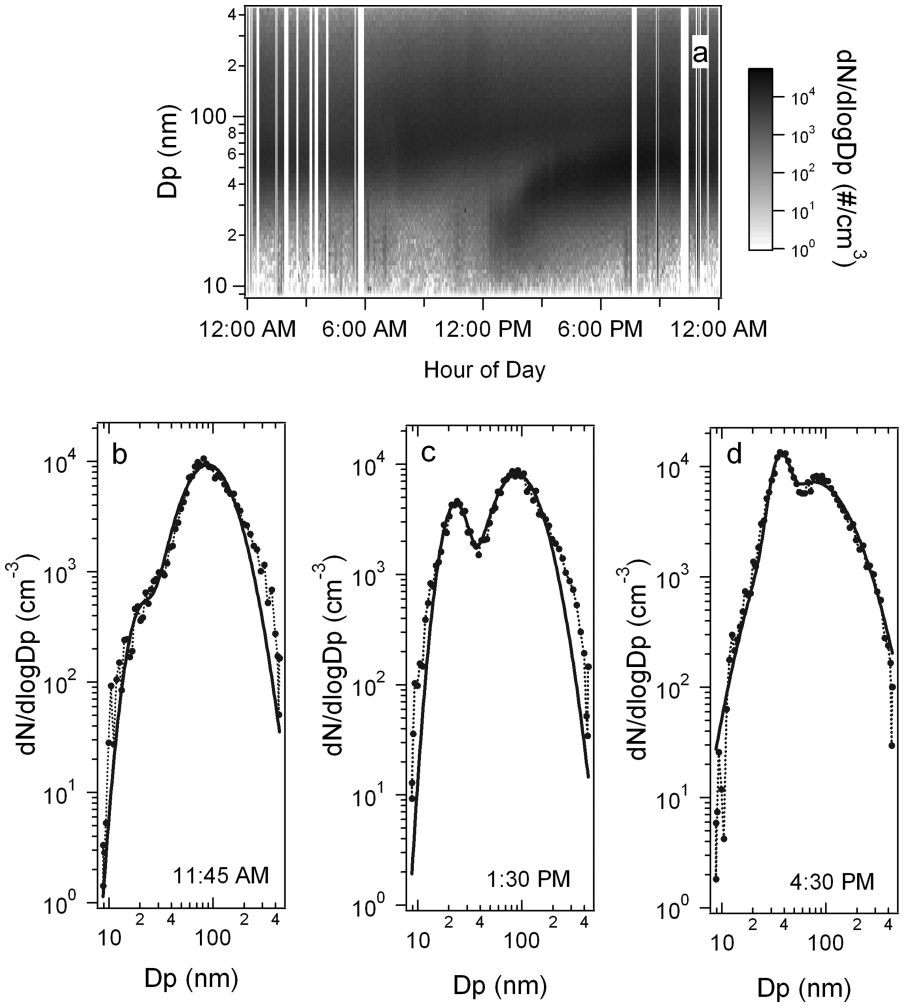

FIG. 5. (a) A typical growth event observed at the Blodgett field site as measured by the SMPS system. The lower plots show individual size distributions, denoted by the line with circles, (b) at the onset of the growth event, (c) during the event, and (d) after significant growth. The results of the fitted bi-modal distribution are superimposed onto the size distributions as a thicker solid line.

At the Blodgett field location, the prevailing winds bring air parcels that have been progressively more affected by anthropogenic emissions and subsequent photochemical processing as the day proceeds. Under these conditions, it is difficult to state that air mass is homogeneous. However, we do think that the biogenic emissions from the forest, and the subsequent photochemical processing of those emissions, do influence the observed growth events. As previously discussed, the wind patterns at the site are extremely consistent during the summer. Following daytime airmass trajectories, the site is located approximately 30 km into the pine forest, preceded by about 10 km of oak forest and savannah. At average wind speeds observed during the day, an air parcel will spend between 4 and 6 hours over forested land before arriving at the Blodgett tower. Furthermore, because the wind does not complete its shift to the northeast until approximately 10 am PST, the site does not experience significant anthropogenic influence for a few more hours. This minimal anthropogenic influence on air parcels in the morning is supported by the diurnal pattern in black carbon, which does not show a significant increase until after 1 pm PST. Since the particle growth events are observed around noon, the photochemistry that influences their growth must occur primarily over the forest. Moreover, the meteorological conditions that appear conducive for nucleation and subsequent growth events occur over large spatial scales.

The following analysis characterizes the daily conditions under which growth events do and do not occur, with an eye towards understanding the meteorological, photochemical, and aerosol conditions that are conducive to the formation and growth of new particles. Some basic characterization of the size distribution behavior during the growth events will be performed; however, attempts to elucidate the probable species responsible for growth will be presented in a separate manuscript.

Growth Event Characterization

Figure 6 shows image plots of two size distributions measured by the SMPS system representing the extremes of the observations at the Blodgett site. Figure 6a shows size distribution data for a day exhibiting a typical aerosol growth event at the site while Figure 6b shows data for a day where no growth occurred. The growth events are distinguished by having slightly different particle sizes at which the nuclei mode particles are detected and the size to which they ultimately grow. To characterize the growth events, the SMPS data were fitted assuming a lognormal size distribution, resulting in a geometric mean diameter (D_{pg}) and geometric standard deviation (σ_g) as a function of time. Both unimodal and bimodal fits were performed, and a goodness of fit parameter was used to assess which provided the better fit. Curves representing the results of the bimodal fits are shown overlaid over the size distribution data in Figure 6. During periods when the growth event occurs, a clear bimodal distribution is seen in the data. This result can be seen in Figure 6a where a sudden sharp drop in the smaller of the two calculated modes occurs, with the fitted D_{pg} decreasing from approximately 100 nm to below 20 nm. This sudden decrease is not seen in Figure 6b. Figure 6b shows a common characteristic of the curve fitting—that the distributions with a single number mode peak could often be better fitted using a bimodal distribution.

The size distribution timelines shown in Figure 6 are fairly easy to characterize, however many days were more ambiguous and the distinction between event and non-event days are often more difficult to detect. Instrument limitations did not allow observation of particles below approximately 10 nm, which means that the particles have already grown a substantial amount from the initial cluster (typically assumed to be around 1 nm) by the time they are observed by the SMPS system. In addition, particle growth was not always observed at the smallest detectable sizes but was often observed to begin between 15 and 20 nm (as determined by the fitted size distribution), with strong growth occuring from that size onward. (Sensitivity to particles less than

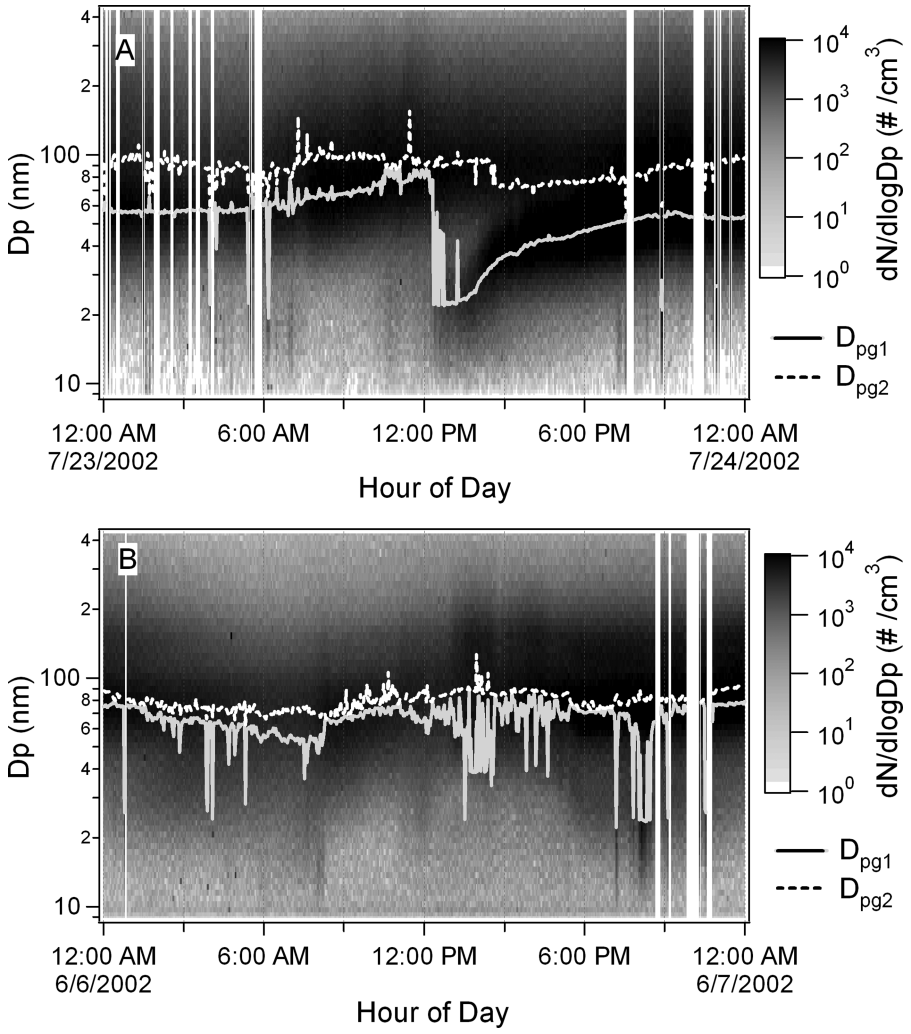

FIG. 6. Size distribution measured as a function of time for (a) a typical day when a growth event occurred and (b) a day when no event occurred. The curves that overlay the images are the results of the bimodal fitting procedures with the larger and smaller modes indicated by the dotted and solid line, respectively.

approximately 15 nm in size was less than desirable.) On a few days, a sustained particle growth is observed for particles that are first detected at around 40 nm. On some days, particles smaller than 40 nm are observed in the afternoon in the size distribution data that do not grow to larger sizes and that only persist for a short period of time before they are presumably advected away. On these days, it appears that the optimum conditions allowing for growth by gas-to-particle condensation are no longer present.

The present experimental system does not allow for the detection of particles at the smallest sizes, hence we cannot unequivocally state that the particle nucleation and growth occur in over the forest. However, we can comment on the degree to which particle growth is affected by atmospheric processing of forest emissions by considering the time scales for particle growth due to different processes. The rate at which particles will grow depends upon the amount of vapor available for condensation, and intramodal coagulation between particles of similar size. In addition, the nuclei mode particles will be lost by coagulation with the larger Aitken mode particles. While condensation is generally considered to be the primary mechanisms responsible for the growth of the nuclei mode particles (Zhang et al. 2004; Kulmala et al. 2004), the time for growth due to coagulation alone provides an upper estimate for particle lifetimes. Based on conditions present at the site, the characteristic lifetime for a 3 nm sized particle to be lost due to coagulation with the existing particle surface area is approximately 0.5 hrs, and that for a 10 nm sized particle increases to approximately 2 hours. Previous investigators have found that it can take from 2.5 to 7 hours from the time when 3 nm sized particles are first detected to grow to a size distribution with a 20 nm number mode peak (Weber et al. 1997; Kulmala et al. 1998, 2004). Other observations in an urban area found faster times of approximately 1 hour for growth from the 3–10 nm range to the 18–33 nm range (Zhang et al. 2004). We previously estimated that the air parcels would spend between 4 and 6 hours over forested land before arriving at the Blodgett experimental site. Given the extent and emissions of the forest upwind of the measurement site, and the large amount of photochemical activity in the region, it is likely that oxidation products of the biogenic emissions will significantly contribute to the growth of the particles observed at the site (Lamanna and Goldstein 1999; Holzinger et al. 2005).

In order to investigate the relationship between the occurrence of growth events and other variables measured at the site, it was necessary to characterize the growth events. A classification system was established similar to that described by Makela et al. (2000), with different days classified with a number ranging from 0 to 3. Classification relied on the results of the uni- and bimodal curve fits to provide data detailing the presence and growth characteristics of the nuclei mode aerosol. Days with no discernable growth event were designated as type 0 while days with a strong appearance of a nuclei-mode aerosol and subsequent growth were designated as type 3. Days where the bimodal curve fit showed a second small mode, often 50 nm or smaller, that did not grow appreciably were characterized as type 1. Finally, days that showed the appearance of a small mode in the size distribution that did not undergo sustained growth or days when the nuclei-mode signal was weak with smaller number concentrations than typically observed, were classified as type 2. The distinction between days was somewhat subjective, particularly between those of type 1 and 2. Classification of days into event types was only performed for days that had enough hours of SMPS data to make a distinction possible. A total of 107 days were classified resulting in 21 days of event type 0, 32 days of event type 1, 21 days of event type 2, and 33 days of event type 3. The days classified as event types 0 and 3, no growth and strong growth, are the focus for the subsequent analysis described below.

Aerosol Patterns and Event Type

With individual days characterized by their event type, the behavior of different variables at the field site can be investigated separately for different event types. Analyses of data that are sorted in this manner help identify conditions that are conducive for the growth of nuclei-mode particles. Figure 7 shows the diurnal profile of total particle number, condensation sink, and volume, as calculated from the SMPS size distributions for days with no growth events (type 0) and with strong growth events (type 3). The condensation sink can be defined as follows (Kulmala et al. 2001)

$$CS = \int_{8nm}^{412nm} D_p \, \beta \, (D_p) \text{ and } n(D_p) \, dD_p \qquad [1]$$

where D_p is the diameter of the particle, $n(D_p)$ is the aerosol size distribution. β is a correction factor that accounts for the decrease in the rate of mass transfer predicted by continuum transport (Fuchs and Sutugin 1970). It is necessary to apply the correction when the particle size approaches that of the mean free path of the gas. The condensing gas was assumed to be pinonic acid, and its binary diffusivity in air was calculated using the empirical formulation of Fuller, Schettler, and Giddings presented in Polling et al. (2000). The values presented in Figure 7 were integrated from 8 nm to 412 nm, the size range measured during the experiment, and is a low estimate for these variables, particularly for the condensational sink and the total aerosol volume.

The diurnal profiles for particle number are similar in shape for days with and without growth events—a minimum in the early morning followed by an increase in the afternoon as anthropogenic pollutants are advected to the site. Days with no growth events show smaller number concentrations than days with growth events. The strong increase in number concentration after noon on growth event days is a reflection of the large increases in particle number concentration that result from nuclei-mode growth events.

The diurnal profiles for the condensation sink show little difference between days with and without growth events. This

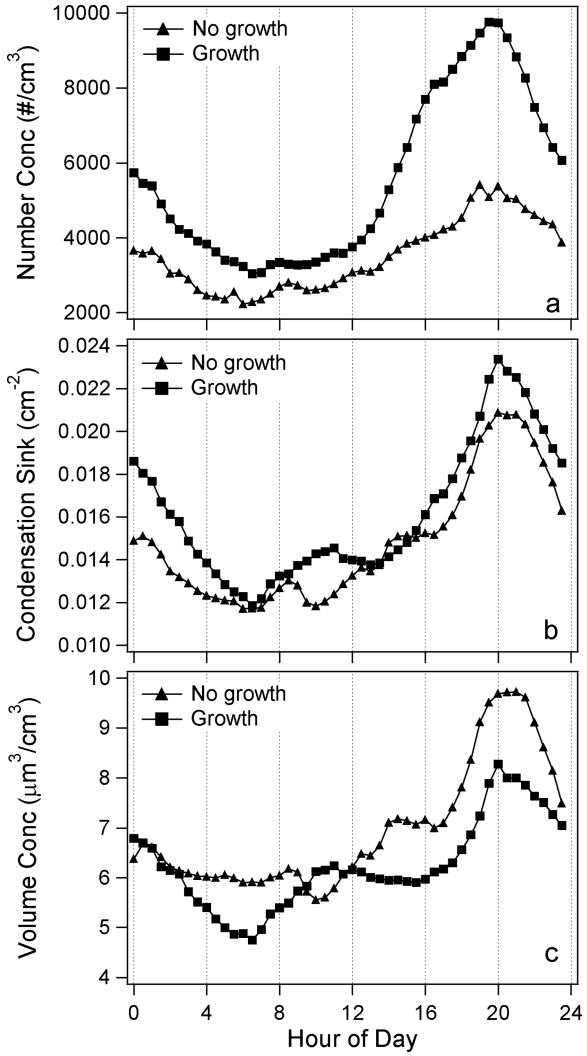

FIG. 7. Mean diurnal pattern of (a) aerosol number, (b) condensational surface area, and (c) volume concentration calculated for the size range 10 to 410 nm from the measured mobility distributions for days with strong growth events (square markers), and days with no observed growth event (triangular markers).

differs from results obtained at other locations that show that particle formation and growth tend to occur on days with decreases in the condensational sink (Stanier et al. 2004; Clement et al. 2001) or total surface area concentration (Weber et al. 1997). Other groups have observed lower values of the condensational sink rate (the condensational surface area multiplied by the binary gas diffusivity) on event days (Buzorius et al. 2003; Vana et al. 2004; Komppula et al. 2003). The formation and subsequent growth of particles in the nuclei mode depend upon the concentration of precursor gases in the atmosphere. These gases are produced photochemically and can be removed by condensation onto pre-existing aerosol surfaces. If the condensational surface area of the aerosol is large enough, it will serve as a significant sink for the condensing gases, suppressing nucleation and growth. Clearly, the magnitude of the condensational sink is important, but vapor production rates are also important. If the latter are high enough, particle growth events can still occur. In the Pittsburgh area, events were observed to occur on days with higher condensational sinks if the production of condensable gases (as indicated by the product of UV intensity and SO_2 concentration) was high enough. It is possible that, at the Blodgett location, the production of precursors is driven by photochemical and other meteorological processes, and therefore the magnitude of the condensational sink is of less importance.

Figure 7c shows that total particle volume tends to be lower on days with growth events when compared to days with no event. There is also a difference in the diurnal profiles between event and non-event days. Days with growth events show a decrease in particle volume in the early morning hours. Particle volume subsequently increases until approximately 1200 PST, and then remains relatively flat until transport from the Sacramento valley results in a large increase in particle volume in the late afternoon. In contrast, particle volume is relatively flat in the morning on days with no growth events, rising just after noon and again in the later afternoon. While there is no readily apparent explanation for the early morning decrease in particle volume, it appears that there are enhanced loss processes in the morning on event days that result in an atmosphere with a lesser aerosol burden on event days.

Table 1 presents three different averages calculated for different time windows; an average calculated during the daytime, when PAR values are greater than 0, an average calculated from sunrise to 1200 PST, and an average calculated from 1200 PST to 1600 PST. Standard deviations are also reported in the table to provide a measure of the range of values observed for each quantity. Averages for the morning period were examined because the observed growth events are initiated in the morning, and thus may be more sensitive to the atmospheric conditions in the morning. The averages calculated during the early afternoon hour, when the majority of the observed particle growth is occurring, may reveal insights into variables affecting the growth process. Table 1 shows that measures of anthropogenic pollution, represented by black carbon and CO, tend to be smaller on days with growth events independent of the averaging time. The average values for total aerosol volume concentration and the measured scattering coefficient, b_{scat}, show that there is more aerosol mass at the site on non-event days, as also shown in Figure 7. The values calculated for both total particle area and condensation sink show no significant difference between event and non-event days during any time period investigated.

The average diurnal behavior of important meteorological variables, as well as black carbon, calculated for days with strong growth events and days with no growth events is shown in Figure 8. These figures augment the data shown in Table 1. Figure 8f illustrates the result that black carbon concentration is greater on non-event days. Note that the morning increase in black carbon on non-event days is larger

TABLE 1

Mean values and standard deviations of the daily averages of aerosol, trace gas, and meteorological variables for event and non-event days calculated for three separate daily time periods

Event type	BC Conc ng/m^3	Bscat Mm^{-1}	Volume conc. μm^3/cm^3	Area conc. μm^2/cm^3	Condens. sink cm^{-2}	CO ppb	O_3 ppb	O_3 flux Total	O_3 flux Surf μmol/m^2/h	O_3 flux Chem	Temp °C	RH %	PAR	Wind speed m/s	Mom. flux N/m^2
Daytime average (PAR > 0)															
No Event	351.6 ± 235	27.9 ± 14.6	7.0 ± 5.1	190.3 ± 106.7	0.014 ± 0.008	245.5 ± 28.8	61.5 ± 12.4	32.6 ± 7.5	18.5 ± 5.3	14.1 ± 4.1	21.2 ± 4.2	34.3 ± 8.7	1004 ± 99	1.75 ± 0.39	0.17 ± 0.07
Str. Event	264.4 ± 149	24.8 ± 11.3	6.2 ± 3.5	195.7 ± 78.3	0.015 ± 0.006	225.2 ± 25.3	59.5 ± 8.4	36.2 ± 10.5	21.4 ± 5.6	14.9 ± 7.0	19.2 ± 3.2	40.3 ± 11.8	1003 ± 130	1.91 ± 0.48	0.21 ± 0.1
Average between sunrise and 1200 PST															
No Event	304.1 ± 217	26.3 ± 14.3	6.0 ± 5.1	160.1 ± 114.6	0.012 ± 0.008	234.8 ± 42.9	53.0 ± 10.5	31.3 ± 9.8	17.2 ± 4.9	14.1 ± 6.2	19.4 ± 4.0	36.5 ± 9.7	997 ± 115	1.64 ± 0.44	0.14 ± 0.07
Str. Event	249.5 ± 139	23.7 ± 10.0	5.5 ± 3.4	165.9 ± 84.3	0.013 ± 0.007	219.3 ± 34.5	55.4 ± 8.4	35.1 ± 10.9	20.6 ± 5.1	14.6 ± 7.2	18.1 ± 3.3	41.8 ± 12.8	1000 ± 117	1.85 ± 0.36	0.18 ± 0.14
Average between 1200 PST and 1600 PST															
No Event	357.5 ± 253	29.2 ± 16.2	6.8 ± 5.5	184.7 ± 114.8	0.014 ± 0.008	254.4 ± 27.8	62.1 ± 11.6	47.7 ± 11.9	26.8 ± 8.6	20.7 ± 7.1	24.0 ± 4.7	29.4 ± 9.3	1488 ± 171	2.32 ± 0.51	0.27 ± 0.1
Str. Event	241.4 ± 190	25.6 ± 16.2	6.0 ± 4.9	178.2 ± 104.6	0.014 ± 0.007	225.6 ± 21.6	60.0 ± 9.4	51.1 ± 17.3	29.9 ± 9.4	21.2 ± 11.7	21.3 ± 3.4	35.0 ± 12.5	1489 ± 266	2.48 ± 0.53	0.33 ± 0.13

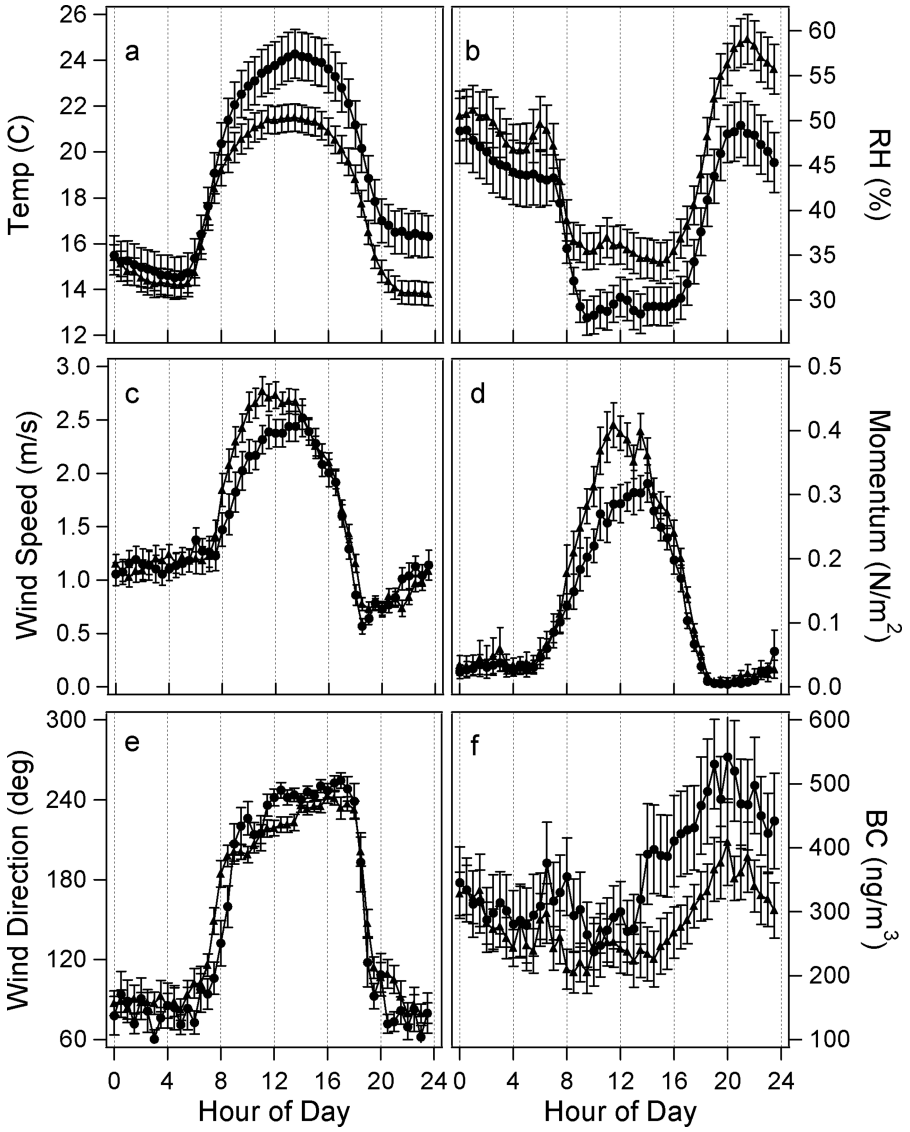

FIG. 8. Mean diurnal pattern of (a) temperature, (b) relative humidity, (c) wind speed, (d) momentum flux, (e) wind direction, and (f) black carbon concentrations for days with no growth event (circular markers) and with growth events (triangular markers).

and persists for a longer period of time than on event days. This increase in anthropogenic influence on non-event days is also reflected in the values of average volume concentration and particle scattering, which are larger on days with no growth event, signifying an atmosphere with more aerosol, which will serve to suppress particle nucleation and growth.

Figure 8a shows that on days when growth events occur, the temperature was lower on average than days that had no growth events. This correlation has been observed in a number of previous studies (Nilsson et al. 2001a; Buzorius et al. 2003; Stainer et al. 2004), and was associated with the passage of a cold front through the area or days with cold air advection. These days in these studies often correspond to clear-sky conditions, and thus larger amounts of radiation available to drive chemistry. As previously discussed, very few days at the Blodgett site had any appreciable cloudiness; thus colder days did not necessarily have increased PAR to drive atmospheric photochemistry. This observation is supported by the results reported Table 1, which show no significant difference in the average value of PAR for event and non-event days for all averaging times. Moreover, average diurnal profiles constructed for event and non-event days (not shown) are identical. If the growth of the nuclei mode particles were due to the condensation of organic oxidation products, temperature would be an important parameter controlling the amount of condensation. The partitioning coefficient for SOA formation is inversely proportional to vapor pressure of the absorbing compound. When the temperature is reduced, more of the oxidation products will partition into the aerosol phase. It is also possible that lower temperatures may result in slower rates for the reactions that produce the

condensable oxidation products, although we expect this effect is minor.

The connection between relative humidity, nucleation, and growth is complex. Relative humidity was larger on days with growth events, as shown in Figure 8b. This is partially attributable to temperatures being lower on event days as well. This result contrasts with previous investigations at forested continental locations that have observed negative correlations between relative humidity and aerosol nucleation (Weber 1997) and lower absolute water vapor concentration (Buzorius 2003). Weber (1997) argues that total particle surface area is correlated with relative humidity, which results in a negative correlation with growth events. However, Buzorius (2003) found only a very slight correlation between relative humidity and condensational surface area. In both cases, the relative humidity was lower than the value at which hygroscopicity significantly affects particle size. Photochemical pathways may also be affected by water vapor concentration, both in terms of reactions producing the incipient nuclei and those controlling the oxidation of molecules responsible for particle growth.

Figures 8c and 8d show that both wind speed and momentum flux are larger on days with strong growth events. The wind direction on event days comes from a more southeasterly direction, illustrated in Figure 8e, changing from an average afternoon direction (calculated between 1200 and 1600 PST) of 245 to 230 degrees. In addition, wind speed and momentum flux increase earlier in the day, and the wind shifts direction about an hour earlier. This correlates with other investigations indicating that nucleation corresponds to days with higher turbulent intensities, strong vertical mixing, and increased heat flux (Buzorius et al. 2003; Nilsson et al. 2001a). The work on Nilsson et al. (2001a) showed a strong correlation between the onset of nucleation and the onset of turbulence. These correlations suggest a connection between the boundary layer dynamics and the onset of nucleation. Nilsson et al. (2001a) suggested several hypotheses for this correlation that involve the production of clusters capable of becoming nuclei upon which observed growth occurs: (1) the mixing could either move clusters from the residual layer into the mixed layer, where they undergo additional growth; (2) the changes in temperature and/or precursor vapor concentration between the entrainment zone and the surface may enhance particle formation; or (3) increased mixing may simply lower the mixed layer aerosol concentration by dilution, enhancing the probability of nucleation. The measurements at the Blodgett location do not allow for further conclusions to be drawn about mechanisms (1) or (2) as both seem possible. The diurnal profiles shown in Figure 7 as well as the data presented in Table 1 show that aerosol concentrations imply that mechanism (3) may be less important, as the total area concentration shown no significant difference between event and non-event days, and total particle volume is only slightly smaller, particularly in the morning when atmospheric conditions that effect the likelihood of an event are established.

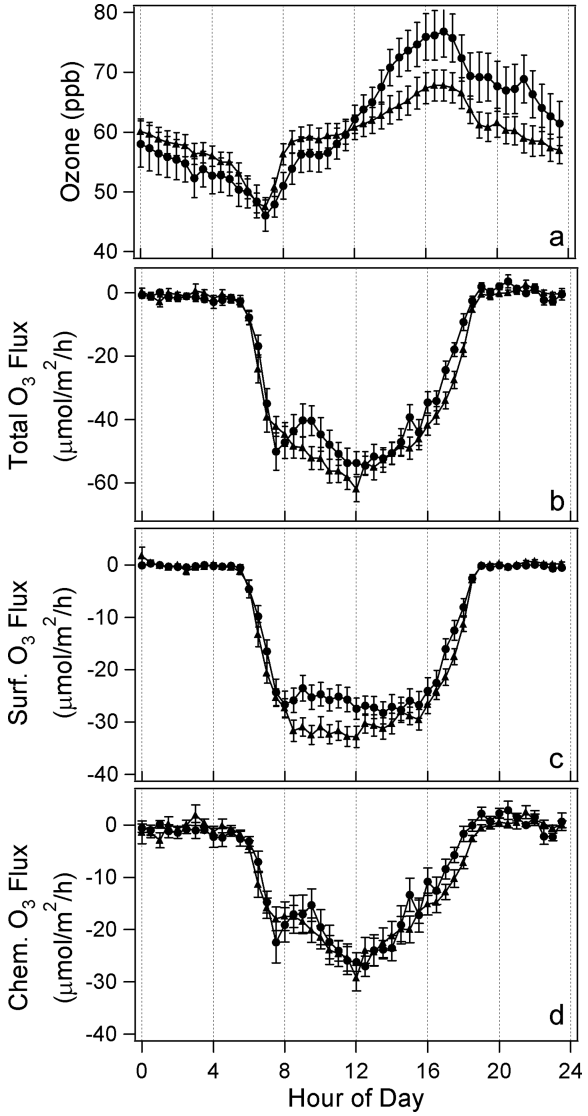

FIG. 9. Mean diurnal pattern of (a) ozone concentration, (b) total ozone flux into the canopy (c) the ozone flux due to surface losses, and (d) the ozone flux due to chemical reactions within the canopy for event days (triangular markers) and non-event days (circular markers).

The diurnal profile for ozone concentration is shown in Figure 9a. Although concentrations are higher in the morning on growth event days, the ozone concentration are generally lower on days with strong formation events. Figure 9 also presents the ozone flux into the canopy for days with and without strong growth events. The negative values for the flux indicate net deposition into the canopy. In addition, the total flux of ozone into the canopy is divided into two components; ozone flux to stomata plus non-stomatal surfaces, and ozone loss due to gas phase chemistry, shown in Figure 9c and 9d (Kurpius and Goldstein 2003). The magnitude of the flux of ozone into the canopy is similar on both event and non-event days (Figure 9b). However, event days have greater ozone flux into the canopy in the morning while non-event days

show a decrease after an early morning peak in total flux. This decreased flux corresponds roughly in time to the rebound in ozone concentration after the morning minimum. There is not a significant difference between the degree of ozone flux due to chemical reactions in the canopy on event and non-event days. The differences between the two total ozone flux curves are due to differences in the stomata plus non-stomatal surface uptake (Figure 9c.) The amount of ozone flux to surfaces, stomatal and non-stomatal, depends upon the water status of the ecosystem (reflected in the values of the soil moisture and the atmospheric vapor pressure deficit), the phenology of the pine trees, and the atmospheric ozone concentration. The stomatal uptake dominates this term, and it is strongly influenced by the atmospheric vapor pressure deficit. As event days tend to have higher values for the relative humidity (Figure 8b), this would lead to higher values for stomatal uptake of ozone during the morning hours. In addition, the ozone concentration is higher in the morning on events days, leading to larger values for surface uptake.

The results presented in Figure 9 show that about half of ozone flux into the forest is due to gas-phase chemical reactions within the canopy (Kurpius and Goldstein 2003; Goldstein et al. 2004). The peak in the flux due to chemical loss in the early morning (approximately 700 PST) is correlated with increased concentrations of highly reactive, light dependent terpene compounds emitted upon sunrise (Lee et al. 2005). Recent gas phase measurements at the site also show additional classes of very reactive biogenic VOCs that are consumed within the canopy, and whose oxidation products are likely to be important in the formation of SOA (Holzinger et al. 2005). These results indicate that ozone is a likely oxidant for the biogenic VOCs emitted by forest, and that the oxidation products of these reactions may be important in the observed growth events. If conditions are favorable and nuclei are present, these products should contribute to the observed growth events.

Growth Rates

Growth rates were calculated for days with a strong growth events (type 3) using the results of the bimodal curve fits as shown on individual size distributions in Figure 5 and for an entire day in Figure 6. As previously discussed, the growth events vary in time of initiation, growth rate, and duration. In order to compare one event to another, average growth rates were calculated for the first 4 hours. The growth rates were calculated using 20-minute averages of SMPS data. Rolling averages of both 1 and 2 hour windows were determined from these 20-minute growth rates, and these rolling averages were averaged to provide an average 4-hour growth rate. A histogram of the resulting growth rates is shown in Figure 10. The resulting rates ranged from 0.76 to 7.36 nm hr^{-1}, with an average of 3.8 nm hr^{-1}. These growth rates are in the range of those observed by other investigators. A recent review of formation

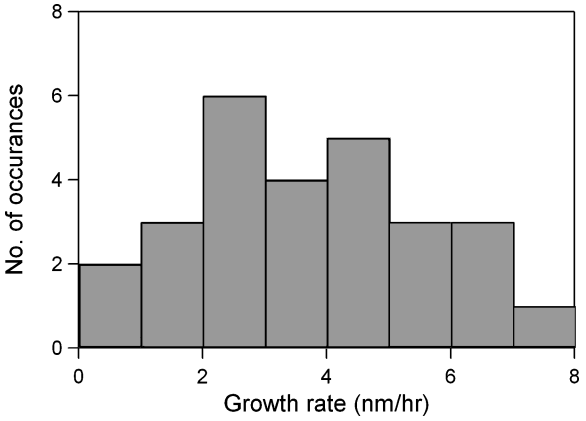

FIG. 10. Histogram of the growth rates calculated for days that exhibit a strong growth event.

and growth of ultrafine atmospheric particles (Kulmala et al. 2004) reported that typical particle growth rates range from 1 to 20 nm hr^{-1} in the midlatitudes, and depend upon the temperature and concentration of available condensable vapor. Growth rates during the summer months at a forested, rural, and urban location were in the range from 4 to 10 nm hr^{-1}.

CONCLUSIONS

Fine particle growth events have been observed at a field site located on the western slope of the Sierra Nevada Mountains of California. This site provides an opportunity to investigate growth events in a rural area that is consistently influenced by anthropogenic emissions advecting to the site from upwind urban areas. During the measurement season, strong particle growth events were observed on 30 percent of the measurement days. Some type of nuclei-mode aerosol was observed on approximately 80 percent of the days, while on many of these days the ultrafine mode did not exhibit the growth behavior that has been seen in many different locations around the globe.

The results show that both meteorology and pollutant concentrations are important for determining days on which growth events are observed. Growth events were observed on days with a lesser degree of anthropogenic influence, as indicated by lower concentrations of BC, CO, and total aerosol volume. An increase in the amount of anthropogenic aerosol at the site serves as a sink for any gaseous oxidation products to condense upon, thereby suppressing nucleation and growth. In addition, growth events tend to occur on days with lower temperatures. These lower temperatures may lead to a larger degree of partitioning of oxidation products to the particle phase, particularly organic oxidation products, as well as lower the barrier for stable nuclei to form in the atmosphere. One of the more interesting findings is a correlation between event days with increased wind speeds and momentum flux measurements. This correlation has been observed by others, and suggests a hypothesis that more vigorous mixing in the atmosphere is an important mechanism behind the

formation of the stable nuclei at the site, upon which additional vapor will condense to produce the observable growth events.

Ozone flux measurements suggest that a large percentage of ozone loss within the canopy is due to gas-phase chemical reactions. Recent gas phase measurements at the site show that very reactive biogenic VOCs are consumed within the canopy, and their oxidation products are likely to be important in the growth of secondary organic aerosols. These observations support the conclusion that condensational growth observed at Blodgett forest is significantly enhanced by the oxidation products of very reactive biogenic VOCs and ozone.

REFERENCES

Becker, E. J., O'Dowd. C. D., Hoell, C., Aalto, P., Makela, J. M., and Kulmala, M. (1999). Organic Contribution to Sub-Micron Aerosol Evolution Over a Boreal Forest—A Case Study, *Phys. Chem. Chem. Phys.* 1:5511–5516.

Bond, T. C. (2001). Spectral Dependence of Visible Light Absorption by Carbonaceous Particles Emitted from Coal Combustion, *Geophys. Res. Letters* 28:4075–4078.

Buzorius, G., Rannik, Ü., Aalto, R., dal Maso, M., Nilsson, E. D., Lehtinen, K. E. J., and Kulmala, M. (2003). On particle Formation Prediction in Continental Boreal Forest Using Micrometeorological Parameters, *J. Geophys. Res.* 108(D13):4337, doi:10.1029/2002JD002850.

Clement, C. F., Pirjola, L., dal Maso, M., Mäkelä, J. K., and Kulmala, M. (2001). Analysis of Particle Formation Bursts Observed in Finland, *J. Aerosol Sci.* 32:217–236.

Collins, D. R., Flagan, R. C., and Seinfeld, J. H. (2002). Improved Inversion of Scanning DMA Data, *Aerosol Sci. Technol.* 36(1):1–9.

d'Almeida, G. A. (1987). On the Variability of Desert Aerosol Radiative Characteristics, *J. Geophys. Res.* 92:3017–3026.

Dillon, M. B., Lamanna, M. S., Schade, G. W., Goldstein, A. H., and Cohen, R. C. (2002). Chemical Evolution of the Sacramento Urban Plume: Transport and Oxidation, *J. Geophys. Res.* 107(D5):doi:10.1029/2001JD000969.

Dreyfus, G. B., Schade, G. W., and Goldstein, A. H. (2002). Observational Constraints on the Contribution of Isoprene Oxidation to Ozone Production on the Western Slope of the Sierra Nevada, California, *J. Geophys. Res.* 107(D19):4565, doi:1029/2001JD001490.

Dunn, M. J., Jimenez, J. L., Baumgardner, D., Castro, T., McMurry, P. H., and Smith, J. N. (2004). Measurements of Mexico City Nanoparticle Size Distributions: Observations of New Particle Formation and Growth, *Geophys. Res. Lett.* 31:L10102, doi:10.1029/2004GL019483.

Fuchs, N. A., and Sutugin, A. G. (1971). *Highly Dispersed Aerosols*. In Topics in Current Aerosol Research (Part 2), edited by G. M. Hidy and J. R. Brock. Pergamon, New York, 1–200.

Goldberg, E. D. (1985). Black Carbon in the Environment: Properties and Distribution, Wiley-Interscience, New York.

Goldstein, A. H, Hultman, N. E., Fracheboud, J. M., Bauer, M. R., Panek, J. A., Xu, M., Qu, Y., Guenther, A. B., and Baugh, W. (2000). Effects of Climate Variability on the Carbon Dioxide, Water, and Sensible Heat Fluxes Above a Ponderosa Pine Plantation in the Sierra Nevada (CA), *Agricultural and Forest Meteorology* 101:113–129.

Goldstein, A. H., McKay, M., Kurpius, M. R., Schade, G. W., Lee, A., Holzinger, R., and Rasmussen, R. A. (2004). Forest Thinning Experiment Confirms Ozone Deposition to Forest Canopy is Dominated by Reaction with Biogenic VOCs, *Geophysical Research Letters* 31(22): L22106, doi:10.1029/2004GL021259.

Gundel, L. A., Dod, R. L., Rosen. H., and Novakov, T. (1984). The Relationship between Optical Attenuation and Black Carbon Concentration for Ambient and Source Particles, *Sci. Tot. Environ.* 36:197–202.

Hansen, A. D. A., Rosen, H., and Novakov, T. (1984). The Aethalometer—An Instrument for the Real-Time Measurement of Optical Absorption by Aerosol Particles, *Sci. Tot. Environ.* 36:191–196.

Hansen, A. D. A., and Rosen, H. (1985). Horizontal Inhomogeneities in the Particulate Carbon Component of the Arctic Haze, *Atmos. Env.* 19(12):2175–2180.

Hering, S. V., Kirby, B. W., Wittig, B., and Magliano, K. (2001). Winter Spatial and Temporal Distribution of Fine Particle Nitrate in the San Joaquin Valley of California, USA, *J. Aerosol Science* 32:S631–S632.

Holzinger, R., Lee, A., McKay, M., and Goldstein, A. H. (2005). Seasonal Variability of Monoterpene Emission Factors for a Ponderosa Pine Plantation in California, *Atmos. Chem. Phys. Disc.* 5:8791–8810.

IPCC (2001). Climate Change 2001: The Scientific Basis: Contribution of Working Group I to the Third Assessment Report of the Intergovernmental Panel on Climate Change. Edited by J.T. Houghton et al., Cambridge Univ. Press, New York.

Jang, M. Czoschke, N. M., Lee, S., and Kamens, R. (2002). *Science* 298:814–817.

Juozaitis, A., Trakumas, S., Girgzdiene, R., Girdzdys, A., Sopauskiene, D., and Ulevicius, V. (1996). Investigations of Gas-to-Particle Conversion in the Atmosphere, *Atmos. Res.* 41:183–201.

Kanakidou, M., Tsigaridis, K., Dentener, F. J., and Crutzen, P. J. (2000). Human-Activity-Enhanced Formation of Organic Aerosols by Biogenic Hydrocarbon Oxidation. *J. Geopys. Res.* 105(D7):9243–9254.

Kavouras, I. G., Mihalopoulos, N., and Stephanou, E. G. (1998). Formation of Atmospheric Particles from Organic Acids Produced by Forests, *Nature* 395:683–686.

Kirchstetter, T. W., Novakov, T., and Hobbs, P. V. (2004). Evidence that Spectral Light Absorption by Aerosols Emitted from Biomass Burning and Motor Vehicles is Different due to Organic Carbon, *J. Geophys. Res.* 109:D21208, doi:10.1029/2004JD004999.

Komppula, M., Lihavainen, H., Hatakka, J., Paatero, J., Aalto, P., Kulmala, M., and Viisanen, Y. (2003). Observations of New Particle Formation and Size Distributions at Two Different Heights and Surroundings in Subarctic Area in Northern Finland, *J. Geophys. Res.* 108(D9):4295, doi:10.1029/2002JD002939.

Kulmala, M., Toivonen, A., Mäkelä, J. M., and Laaksonen, A. (1998). Analysis of the Growth of Nucleation Mode Particles Observed in Boreal Forest. *Tellus*, 50B:449–462.

Kulmala, M., Dal Maso, M., Mäkelä, J. M., Pirjola, L., Väkevä, M., Aalto, P., Miikkulainen, P., Hämeri, K., and O'Dowd, C. D. (2001). On the Formation, Growth and Composition of Nucleation Mode Particles, *Tellus* 53B:479–490.

Kulmala, M., Korhonen, P., Napari, I., Karlsson, A., Berresheim, H., and O'Dowd, C. D. (2002). Aerosol Formation During PARFORCE: Ternary Nucleation of H2SO4, NH3, and H20, *J. Geophys. Res.* 107(D19):8111, doi:10.1029/2001JD000900.

Kulmala, M., Vehkamäki, H., Petäjä, T., Dal Maso, M., Lauri, A., Kerminen, V. -M., Birmili, W., and McMurry, P. H. (2004). Formation and Growth Rates of Ultrafine Atmospheric Particles: A Review of Observations, *J. Aerosol Sci.* 35:143–176.

Kurpius, M. R., McKay, M., and A. H. Goldstein. (2002). Annual Ozone Deposition to a Sierra Nevada Ponderosa Pine Plantation, *Atmos. Env.* 36:4503–4515.

Kurpius, M. R., and A. H. Goldstein. (2003). Gas-Phase Chemistry Dominated O3 Loss to a Forest, Implying a Source of Aerosols and Hydroxyl Radicals to the Atmosphere, *Geophys. Res. Lett.* 30(7):1371, doi:10.1029/2002GL016785.

Lamanna, M. S. and Goldstein, A. H. (1999). In-Situ Measurements of C2–C10 VOCs Above a Sierra Nevada Ponderosa Pine Plantation, *J.Geophys. Res.* 104:21247–21262.

Lee, A., Schade, G. W., Holzinger, R., and Goldstein, A. H. (2005). A Comparison of New Measurements of Total Monoterpene Flux With Improved Measurements of Speciated Monoterpene Flux, *Atmosospheric Chemistry and Physics*, 5:505–513.

Lunden, M. M., Revzan, K. L., Fischer, M. L., Thatcher, T. L., Littlejohn, D., Hering, S. V., and Brown, N. J. (2003). The Transformation of Outdoor Ammonium Nitrate Aerosol in the Indoor Environment, *Atmos. Environ.* 37:5633–5644.

Mäkelä, J. M., Aalto, P., Jokinen, V., Pohja, T, Missinen, A., Palmroth, S., Markkanen, T., Seitsonen, K., Lihavainen, H., and Kulmala, M. (1997). Observations of Ultrafine Particle Formation and Growth in Boreal Forest, *Geophys. Res. Let.* 24(10):1219–1222.

McMurry, P. H., and Wilson, J. C. (1982). Growth Laws for the Formation of Secondary Ambient Aerosols: Implications for Chemical Conversion Mechanisms, *Atmos. Env.* 16(1):121–134.

Mission, L., Lunden, M. M., McKay, M., and Goldstein, A. H. (2005). Atmospheric Aerosol Light Scattering and Surface Wetness Influence the Diurnal Pattern of Net Ecosystem Exchange in a Semi-Arid Ponderosa Pine Plantation, *Agricultural and Forest Meteorology* 129:69–83.

Molenar, J. F., Dietrich, D. L., and Tree, R. M. (1989). In *Visibility and Fine Particles*, Mathai, C. V., Ed., 374–383. Air and Waste Management Association, Pittsburgh.

Nilsson, E. D., Rannik, Ü., Kulmala, M., Buzorius, G., and O'Dowd, C. D. (2001a). Effects of Continental Boundary Layer Evolution, Convection, Turbulence and Entrainment, on Aerosol Formation, *Tellus* 53B:441–461.

Nilsson, E. D., Paatero, J., and Boy, M. (2001b). Effects of Air Masses and Synoptic Weather on Aerosol Formation in the Continental Boundary Layer, *Tellus* 53B:462–478.

O'Dowd, C. D., McFiggans, G., Greasey, D. J., Pirjola, L., Hoell, C., Smith, M. H., Allan, B. J., Plane, J. M. C., Heard, D. E., Lee, J. D., Pilling, M. J., and Kulmala, J. (1999). On the Photochemical Production of New Particles in the Coastal Boundary Layer. *Geophys. Res. Let.* 26:1707–1710.

O'Dowd, C. D., Aalto, P., Hameri, K, Kulmala, M., and Hoffman, T. (2002). Atmospheric Particles from Organic Vapors. *Nature* 416:497.

Poling, B. E., Prausinitz, J. M., and O'Connell, J. P. (2000). *Properties of Gases and Liquids*. 5th edition. McGraw-Hill, New York.

Seinfeld, J., and Pandis, S. (1998). *Atmospheric Chemistry and Physics*. John Wiley & Sons, New York.

Stainer, C. O., Khlystov, A. Y., and Pandis, S. N. (2004). Nucleation Events During the Pittsburgh Air Quality Study: Description and Relation to Key Meteorological, Gas Phase, and Aerosol Parameters, *Aerosol Sci. Tech.* 38(S1):253–264.

Stolzenburg, M. R., and Hering, S. V. (2000). Method for the Automated Measurement of Fine Particle Nitrate in the Atmosphere, *Environ. Sci. Technol.* 34:907–914.

Vana, M., Kulmala, M., Dal Maso, M., Hõrrak, U., and Tamm, E. (2004). Comparative Study of Nucleation Mode Aerosol Particles and Intermediate Ions Formation Events at Three Sites, *J. Geophys. Res.* 109:D17201, doi:10.1029/2003JD004413.

Wang, S. C., and Flagan, R. C. (1990). Scanning Electrical Mobility Spectometer, *Aerosol Sci. Technol.* 13:230–240.

Weber, R. J., Marti, J. J., McMurry, P. H., Eisele, F. L., Tanner, D. J., and Jefferson, A. (1997). Measurements of New Particle Formation and Ultrafine Particle Growth Rates at a Clean Continental Site, *J. Geophys. Res.* 102(D4):4375–4385.

Weber, R. J., McMurry, P. H., Mauldin,L., Tanner, D., Eisele, F., Clarke, A. D., and Kapustin, V. N. (1999). New Particle Formation in the Remote Troposphere: A Comparison of Observations at Various Sites, *Geophy. Res. Lett.* 26:307–310.

Woo, K. S., Chen, D. R., Pui, D. Y. H., and McMurry, P. H. (2001). Measurements of Atlanta Aerosol Size Distributions: Observations of Ultrafine Particle Events, *Aerosol Sci. Tech.* 34:75–87.

Yu, F., and Turco, R. P. (2000). Ultrafine Aerosol Formation Via Ion-Mediated Nucleation. *Geophys. Res. Let.* 27:883–886.

Zhang, K. M., and Wexler, A. S. (2002). A Hyphothesis for Growth of Fresh Atmospheric Nuclei, *J. Geophys. Res.* 107:4577, doi:10.1029/2002JD002180.

Zhang, Q., Stainer, C. O., Canagaratha, M. R., Jayne, J. T., Worsnop, D. R., Pandis, S. N., and Jimenez, J. L. (2004). Insights Into the Chemistsry of New Particle Formation and Growth Events in Pittsburgh Based on Aerosol Mass Spectrometry, *Environ. Sci. Technol.* 38:4797–4809.